Proc. NIPR Symp. Antarct. Meteorites, **8**, 237–249, 1995

ELEMENT DISTRIBUTIONS IN METALLIC FRACTIONS OF AN ANTARCTIC ORDINARY CHONDRITE ALH-77231 (L6)

Ping KONG[1], Mitsuru EBIHARA[1]*, Kazutoyo ENDO[2] and Hiromichi NAKAHARA[1]

[1]*Department of Chemistry, Faculty of Science, Tokyo Metropolitan University, Hachioji-shi, Tokyo 192-03*
[2]*Faculty of Pharmacy, Showa College of Pharmaceutical Sciences, Machida-shi, Tokyo 194*

Abstract: A chemical dissolution method based on different leaching rates of kamacite, taenite and tetrataenite in concentrated HF was developed for isolating metal phases from non-magnetic minerals (mainly silicates) in chondritic meteorites, and for separating taenite from kamacite. This method was applied to an Antarctic chondrite, ALH-77231(L6), to study the elemental distributions between metal and non-magnetic phases and between taenite and kamacite. The separated phases as well as the bulk metal were studied by Mössbauer spectrometry and by INAA.

Mössbauer spectra of ^{57}Fe show that our procedure is efficient in removing silicates from metal and separating taenite from kamacite. The existence of tetrataenite and the absence of disordered taenite in ALH-77231 metals imply that the parent body of ALH-77231 has not experienced severe shock events that redistribute elements among different phases. Thus, element distributions among different phases reflect, in general, the metamorphic history of ALH-77231.

INAA results show that siderophile elements are differently distributed between taenite and kamacite. Most siderophiles have very strong to moderate affinities to taenite, while Co is enriched in kamacite. Refractory siderophile elements seem to behave as an individual group. Distribution of Ir between the metal and the non-magnetic fractions implies that a portion of Ir is present in the silicate fraction. This portion of Ir cannot be attributed to the contamination of FeNi metal in the silicates. While the Os/Ir ratios in the metals of ALH-77231 are in agreement with the CI value, the Re/Ir ratios are significantly higher than the CI value, indicating that Re is fractionated from Ir and Os, between the metal and the non-magnetic fractions. This may be attributable to either the later redistribution of Re between metal and non-magnetic fractions or differences in the condensation phases for Re, and for Ir and Os.

1. Introduction

Kamacite is α-iron with a body-centered cubic (bcc) structure, and taenite is γ-iron with a face-centered cubic (fcc) structure. According to the Fe-Ni phase diagram, the only stable metal phase at temperature higher than 900°C is γ-iron; as the temperature falls from 900°C, α-iron is exsolved from γ-iron and they coexist stably at low temperature (GOLDSTEIN and OGILVIE, 1965).

In most iron meteorites, kamacite and taenite grow with a geometric orientation parallel to each plane and form a specific crystallographic pattern (Widmanstätten pattern) during the cooling process of iron meteorites. GOLDSTEIN and OGILVIE (1965)

*To whom correspondence should be addressed.

pointed out that the Widmanstätten pattern can provide information concerning the thermal histories of iron meteorite parent bodies. Kamacite and taenite are the major metallic phases in ordinary chondrites, but are usually found separated from each other, in individual pure alloy grains (WOOD, 1967). In taenite, Ni contents are highly variable from the rim to the center of the crystals, and the variation changes with sizes of the metal grains. WOOD (1967) interpreted this observation as a result of exsolution of kamacite from taenite, followed by diffusion of Ni into the taenite crystals which effectively ceases upon cooling through 550°C–450°C.

Three methods have been developed for evaluating the cooling rates of meteorite parent bodies on the basis of the specific structures of the kamacite and taenite grown: (i) central Ni content (GOLDSTEIN and OGILVIE, 1965), (ii) profile matching (SAIKUMAR and GOLDSTEIN, 1988), and (iii) kamacite band (NARAYAN and GOLDSTEIN, 1985). All of these models are based on Ni contents and gradients in the metal phases or metal lamellae, which can be obtained by electron microprobe analysis. Recently, the grain-based cooling rates, which were obtained from the metal grains embedded in silicate inclusions, were compared with the cooling rates from Widmanstätten structure for IAB meteorites, in which both types of metals are present (HERPFER *et al.*, 1994). The consistency of cooling rates from the two methods suggests that the occurrence of taenite and kamacite in the chondritic inclusions of IAB irons is diffusion-controlled.

RAMBALDI (1976, 1977a, b) studied trace element distributions in different sizes of metal grains separated from ordinary chondrites and found that siderophile elements are distributed differently between fine-grained metals, corresponding to taenite, and coarse-grained metals, corresponding to kamacite. The distribution trends of siderophile elements in taenite and kamacite must be controlled by their chemical properties, condensation processes and/or thermal histories which the meteorite parent bodies experienced. It remains unclear whether the distributions of trace siderophile elements among the metal phases are controlled by diffusion.

In this study, we developed a chemical dissolution method to separate, first, metal from silicate, and then taenite from kamacite. This method was applied to an Antarctic ordinary chondrite ALH-77231 (L6). The separated metals were studied by INAA and by Mössbauer spectroscopy. On the basis of INAA data and Mössbauer spectra for these metal separates, we evaluated the distribution of siderophile elements between taenite and kamacite. Our final goal is to develop a new method to evaluate thermal histories of ordinary chondritic parent bodies.

2. Experimental

2.1. Sample preparation

Several chips (total weight: 767 mg) of an Antarctic meteorite ALH-77231 (L6) were ground in an agate mortar. The magnetic fraction was first separated by a hand magnet and divided into four portions. As a considerable amount of silicate remained attached to the magnetic fraction, these were dissolved by boiling in conc. HF acid. For the examination of dissolution behaviors of metal alloys, the four portions of magnetic separates were treated in conc. HF acid for different periods: 2, 5, 10 and 15

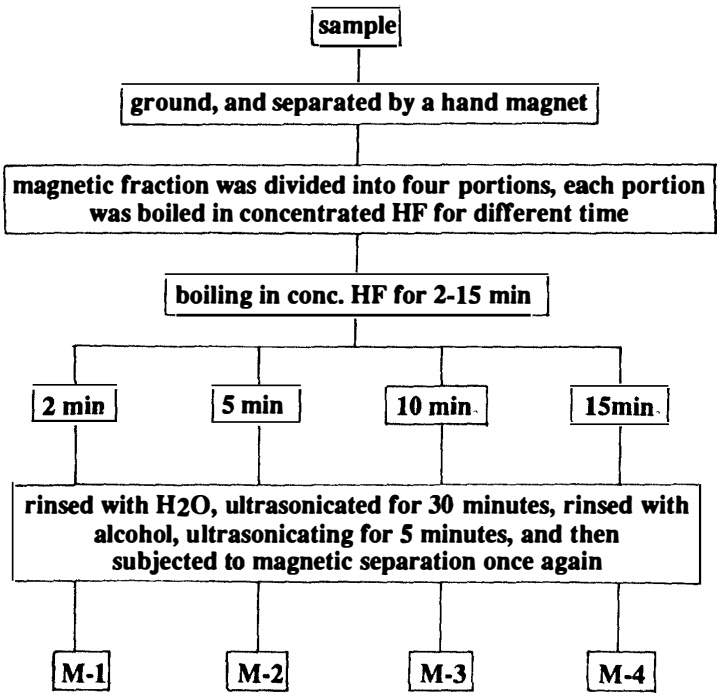

Fig. 1. Schematic procedure for the separation of metallic fractions from ALH-77231.

min. The metal separates were named M1 to M4 corresponding to the leaching time of 2 min to 15 min. The separation scheme is shown in Fig. 1.

2.2. Mössbauer spectrum

Mössbauer spectroscopy was carried out for the metal separates from ALH-77231 at room temperature by using a conventional Mössbauer spectrometer with a ^{57}Co/Rh (370 MBq) source. The velocity was calibrated with the sextet absorption peaks of a pure iron foil, and isomer shift values were normalized to those of metallic iron. A typical measuring time for one metal separate was one week.

2.3. Instrumental neutron activation analysis (INAA)

Trace element contents in the bulk, metal separates, and the non-magnetic fraction of ALH-77231 were determined by INAA. Chemical standards were prepared from highly pure chemical reagents of the elements of interest. The samples were first irradiated for 100 s in the TRIGA-II reactor of Rikkyo University at a neutron flux of 1.5×10^{12} cm^{-2}s^{-1} for the determination of Ge, Rh, Mg, Cu, V, Al and Ca, followed by 6 hours at the same neutron flux for the measurement of Au, Pt, Re, As, Sb, Ga, Pd, Os, Ir, Ni, Fe, Se, Sc and Co. The detailed INAA procedures for the determination of trace siderophiles in chondritic metals will appear elsewhere.

3. Results and Discussions

3.1. Leaching behavior of metals

Our preliminary experiment showed that pure iron can be partly dissolved in conc. HF (Table 1). It was also observed that silicates were more effectively removed from the metal separate in conc. HF at higher temperature. Thus, for obtaining the representative metals with low erosion, 2 min boiling in conc. HF was chosen for M-1 of ALH-77231. Although M-1 was the least severely treated metal separate, no silicates were observed under the microscope, and no Fe-containing silicates or troilite were detected in its Mössbauer spectrum. Thus, the HF treatment is effective for the removal of silicates from the magnetic separate, but it is not clear to what extent the remaining metal is representative of the bulk metal composition. There are two reasons to believe that the composition of this metal is not significantly changed from the original sample. First, a pure iron reagent was used in the preliminary experiment (Table 1), whereas kamacite in meteorites contains about 5–7 wt% of Ni. As Ni metal is much less affected by HF, the dissolution of kamacite is expected to be reduced from the ten percent level. Second, the iron reagent (powder) is in the size range of 0.1–0.15 mm, while the kamacite grains separated from meteorites are generally coarser. The dissolution of kamacite is accordingly lowered compared with the dissolution of pure iron. Therefore, the least treated metal M-1 can be representative of the bulk metal in composition within an error of 5–10%.

As Fe metal is more easily dissolved than Ni metal in conc. HF, it remains unclear whether the fractionation of Ni from Fe occurs when the metal separates are boiled in conc. HF acid. If the HF acid attacks Fe selectively, contents of Fe (and Ni) in the residue should be dependent on the leaching time. The Ni contents in the four metal separates (M-1 to M-4) determined by INAA are shown in Table 3. There seems to be no obvious correlation between the leaching time and the Ni contents in M-2, M-3 and M-4. The Mössbauer spectrum of M-4 in Fig. 2 shows similar transmission intensities of kamacite and paramagnetic taenite. If M-4 results from the M-1 composition, about 90% of the α-phase in the M-1 fraction needs to be dissolved. Assuming that the mean content of Ni in the paramagnetic taenite and tetrataenite is 45%, the Ni content of M-4 is calculated to be 46 wt% if only Fe is selectively leached. This value is also applicable when Ni is reduced after complete dissolution of kamacite. On the other hand, the Ni content is calculated to be 36 wt% if Ni is present

Table 1. Dissolution of Fe metal (in wt%) in conc. HF.*

Temperature (°C)	Time (min)					
	2	5	10	15	20	30
100	16.2	74.4	98.9			
25	11.7	21.4	40.6	56.4	68.1	83.5

* Electrolytic Fe metal (powder) (purity: 99.9%; grain size: 0.1–0.15 mm).

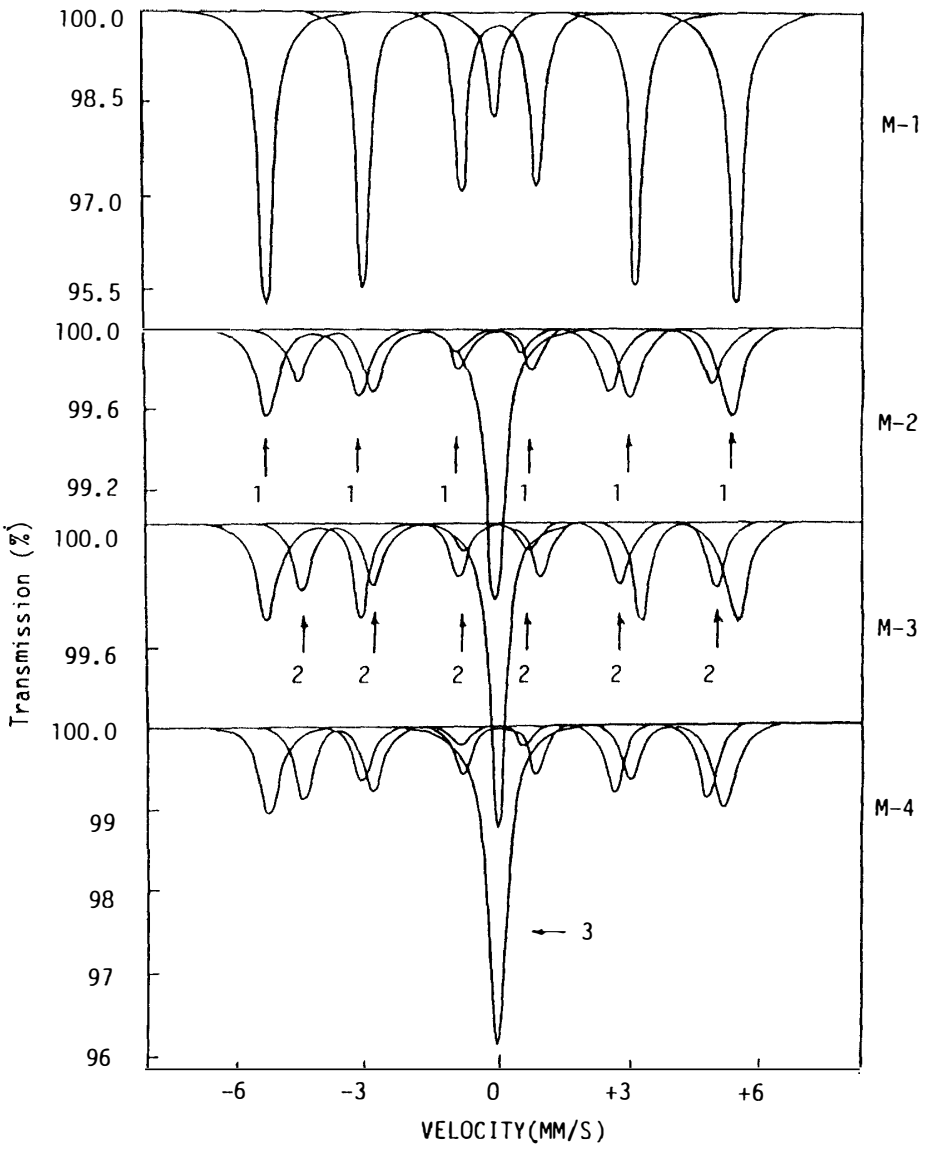

Fig. 2. Mössbauer spectra for the metal fractions of ALH-77231 (1. α-phase, 2. ordered γ-phase, 3. paramagnetic γ-phase).

in the acid solution after decomposition of kamacite. The measured value of 35 wt% (see discussion below) is consistent with the latter. Thus, during the decomposition of kamacite, selective dissolution of Fe or reprecipitation of Ni apparently did not occur.

The question of how the trace siderophile elements in kamacite behave during the dissolution of kamacite may also arise. If any of these elements precipitate in the remaining metals, their abundances in these metals, relative to those in the bulk metal, must be larger than that for Ni. However, our INAA results show an opposite trend for all elements except Cu, which we discuss separately below. Clearly, during the dissolution of kamacite, trace siderophile elements in the kamacite are expected to remain in the acid solution.

According to Mössbauer spectrometry, the M-1 fraction is composed mostly of

Table 2. Mössbauer parameters for metal separates from ALH-77231.

Sample	Phase	Mössbauer parameter*				
		Γ (mm/s)	IS (mm/s)	ΔEq (mm/s)	HF (kOe)	A (%)
M-1	α-phase	0.37	0.01	0.00	339	93
	paramag. γ-phase	0.38	−0.10	—	—	7
M-2	α-phase	0.48	0.03	0.00	335	47
	paramag. γ-phase	0.51	−0.03	—	—	27
	ordered γ-phase	0.46	0.00	0.47	297	26
M-3	α-phase	0.46	0.01	0.00	330	46
	paramag. γ-phase	0.40	−0.06	—	—	26
	ordered γ-phase	0.43	0.00	0.10	289	28
M-4	α-phase	0.48	−0.11	0.00	330	38
	paramag. γ-phase	0.51	−0.08	—	—	31
	ordered γ-phase	0.44	0.00	0.19	291	31

*Γ: the linewidth at half peak height; IS: the isomer shift relative to ^{57}Co/Rh source; ΔEq: the quadrupole splitting; HF: the internal hyperfine field; A: the relative spectral area (in vol %).

α-FeNi, with a relative intensity of 93%; the M-2, M-3 and M-4 fractions are similar, being enriched with paramagnetic-taenite and tetrataenite (Fig. 2 and Table 2). This shows that kamacite can be largely removed by boiling for 5 min in conc. HF but that taenite and tetrataenite are not affected even after boiling for up to 15 min. Thus, on the basis of different leaching rates of kamacite, taenite and tetrataenite in conc. HF acid, taenite and tetrataenite can be selectively enriched. Part of the α-phase is still present in the metal fraction M-2 after boiling in HF for 5 min. This α-phase apparently resists the HF attack, as indicated by the small change of its abundance in M-2, M-3 and M-4. This α-FeNi may be either martensite, which may be less effectively dissolved, or kamacite, which is embedded in the taenite lamellae and has little chance to make contact with the HF during the dissolution.

3.2. Mössbauer spectroscopy

All the Mössbauer spectra for M1 to M4 show a central single peak (Fig. 2), which corresponds to the paramagnetic γ-phase. The paramagnetic γ-phase is formed when a high-temperature Fe-Ni phase, austenite, is incompletely transformed through cooling. Austenite is a solid solution of carbon (or nitrogen) in the γ-phase. A single peak appears if the concentrations of these impurities (C and/or N) are too low to change the symmetry of the metal structure. If the impurity concentrations are increased (*e. g.*, to several %), the high symmetry is lost and a quadruple doublet with a small isomer shift is obtained in place of the single central line (GUTLICH *et al.*, 1978). Thus, concentrations of carbon and nitrogen in the metal separates of ALH-77231 are expected to be less than one wt%.

Tetrataenite (CLARKE *et al.*, 1980; SCORZELLI *et al.*, 1993), an ordered Fe-Ni phase, has a 50-50 Fe-Ni composition. This superstructure (expressed as $L1_0$) is

reported to be produced only by either neutron or electron irradiation of the disordered Fe-Ni alloy under laboratory conditions (REUTER *et al.*, 1989a) but it is commonly present in meteorites (CLARKE *et al.*, 1980; REUTER *et al.*, 1989b; SCORZELLI *et al.*, 1994). As meteorites have cooled at slow rates (~1°C/10^6 years), low-temperature phase transformations (*e.g.*, to ordered Fe-Ni) are expected to have occurred (REUTER *et al.*, 1989b). Due to its low abundance in the metals of ALH-77231, tetrataenite could not be confirmed in the spectrum of M-1. The Mössbauer spectrum of tetrataenite is characterized by its quadruple splitting of about 0.25 mm/s and hyperfine field of 290 kOe (SCORZELLI *et al.*, 1994). After the removal of kamacite from the metal separates, tetrataenite is enriched as inferred by an asymmetric six-line in the spectra of M-2, M-3 and M-4 (Fig. 2).

It is suggested that the ordering-disordering transformation of Fe-Ni alloy took place at a critical temperature of about 320°C (REUTER *et al.*, 1989a; LARSEN *et al.*, 1982). Even though meteorites cooled in the temperature range from 700°C to 200°C for more than 10^8 years, thermodynamic equilibrium of metals has not been totally reached (REUTER *et al.*, 1989a, b). Thus, once the ordered-metal is heated over the critical temperature when being impacted and the ordering-disordering transformation occurs, little ordered-metal structure is reproduced because the cooling rate must be very high. Accordingly, it is expected that while an ordered Fe-Ni phase can preserve the cooling history of a meteorite parent body, the existence of disordered taenite can tell us something about a later heating event (*e.g.*, shock event) on a meteorite parent body. As seen in Fig. 2, tetrataenite is obviously present in ALH-77231, whereas disordered taenite is not; the Mössbauer line of disordered Fe-Ni (50-50) is characterized by a hyperfine field of 310 kOe (LARSEN *et al.*, 1982). The existence of disordered taenite can also be confirmed by the line broadening of tetrataenite, which is described by Γ in Table 2. There seem to be no obvious broadening trends for tetrataenite. Therefore, ALH-77231 does not seem to have experienced shock events which heat it over 320°C. Under these low temperatures, redistribution of elements among different phases cannot occur. Thus, indigenous element distributions between kamacite and taenite can be discussed for ALH-77231.

3.3. Element distributions between taenite and kamacite

The elemental abundances of the bulk, the non-magnetic, and the metal fractions (M-1 to M-4) of ALH-77231.51 determined by INAA are summarized in Table 3, along with the data for Odessa and Allende. The literature data for these two meteorites are also given for comparison. According to the contents of several elements in M-1 and in the non-magnetic silicates, coupled with a weight ratio of the metal to the non-magnetic fraction of 0.096, the bulk contents for ALH-77231 were calculated and are listed in Table 4. These results show that the calculated bulk contents are lower in Ni and higher in Co relative to the analyzed ones, suggesting that the composition of M-1 slightly deviates from the bulk metal of ALH-77231, with the former being enriched with kamacite. Considering the small mass of M-1 (7.7 mg), sample heterogeneity may be an explanation for such a deviation.

Distributions of siderophile elements between taenite and kamacite are listed in Table 5. These are defined as the mean contents of the elements in M-2, M-3 and M-4

Table 3. INAA data (in ppm, unless otherwise indicated) for bulk and metal separates of Antarctic ordinary chondrite ALH-77231 (L6).*

	Odessa		Allende		Bulk	M-1	M-2	M-3	M-4	Non-magnetic
	#	lit.†	#	lit.†						
Weight (g)	0.0199		0.0329		0.0415	0.0077	0.0067	0.0047	0.0039	0.0733
Al(%)	N.D.$^{\Delta}$		1.83 (3.7%)	1.74	1.14 (3.7%)	N.D.	N.D.	N.D.	N.D.	1.39 (3.6%)
As	≡12$^{\$}$ (1.3%)		1.34 (4.2%)	0.8–3	1.1 (13%)	16.7 (2.2%)	15.2 (2.0%)	14.8 (3.3%)	14.8 (3.2%)	N.D.
Au	1.83 (1.1%)	1.68	0.170 (2.6%)	0.15	0.147 (3.9%)	1.66 (1.3%)	5.10 (1.0%)	4.26 (1.0%)	4.90 (1.0%)	<0.008
Ca(%)	N.D.		≡1.85		0.98 (10%)	N.D.	N.D.	N.D.	N.D.	1.41 (9.2%)
Co	4210 (2.7%)		595 (1.4%)	600	586 (0.7%)	6840 (1.0%)	2660 (1.1%)	3580 (2.0%)	2850 (1.0%)	83.5 (0.9%)
Cu	355 (3.7%)		N.D.	119	N.D.	626 (4.2%)	N.D.	4010 (2.3%)	4590 (2.7%)	N.D.
Fe(%)	92.1 (2.4%)		22.7 (1.6%)	23.6	20.9 (2.2%)	89.2 (2.3%)	59.0 (2.5%)	67.7 (2.4%)	63.4 (2.5%)	16.3 (1.6%)
Ge	≡285 (7.6%)		N.D.	11–17.9	N.D.	41 (11%)	160 (11%)	146 (8.6%)	123 (8.2%)	N.D.
Ir	2.32 (2.4%)	1.9	0.70 (12%)	0.74	0.512 (1.5%)	4.65 (2.0%)	14.3 (2.0%)	12.0 (2.1%)	11.0 (2.0%)	0.126 (3.2%)
Mg(%)	N.D.		15 (12%)	14.8	12 (13%)	0.74 (5.2%)	N.D.	0.16 (13%)	0.13 (18%)	13 (19%)
Ni(%)	8.04 (2.5%)	7.3	1.52 (1.4%)	1.42	1.31 (2.1%)	9.98 (2.5%)	40.1 (2.5%)	30.7 (2.5%)	35.3 (2.4%)	0.164 (2.1%)
Os	2.53 (6.8%)	2.6	0.88 (21%)	0.4–0.77	N.D.	5.02 (7.2%)	14.9 (5.5%)	10.5 (9.7%)	11.1 (4.9%)	N.D.
Pt	5.4 (12%)	6.12	N.D.		N.D.	8.4 (18%)	18.6 (6.7%)	16.5 (6.9%)	17 (20%)	N.D.
Re	0.25 (6.5%)	0.23	N.D.	0.06	N.D.	0.512 (4.1%)	1.43 (5.1%)	1.43 (5.3%)	1.05 (11%)	N.D.
Rh	1.49 (9.5%)	1.3	N.D.		N.D.	1.5 (23%)	N.D.	5.6 (13%)	5.78 (8.9%)	N.D.
Sb	0.560 (8.4%)		N.D.	0.08	N.D.	0.61 (20%)	2.00 (5.5%)	2.09 (6.1%)	2.1 (11%)	N.D.
Sc	N.D.		≡11 (0.3%)		8.02 (0.6%)	N.D.	N.D.	N.D.	N.D.	8.76 (0.7%)
Se	N.D.		≡9		8.4 (10%)	N.D.	N.D.	N.D.	N.D.	8.89 (7.5%)
V	N.D.		≡90		59.0 (9.8%)	N.D.	N.D.	N.D.	N.D.	87.8 (8.7%)
Zn	N.D.		116 (9.0%)	110	46 (10%)	N.D.	N.D.	N.D.	N.D.	63 (12%)

*: Values in parentheses are errors due to counting statistics (1 σ). N.D. means "not determined".
#: This work.
†: Literature values; Odessa: HONDA *et al.* (1991), Allende: JAROSEWICH *et al.* (1987).
$^{\Delta}$: Below detection limit.
$: Used as standard.

Table 4. Comparison of some calculated siderophile contents (in ppm, unless otherwise indicated) with analyzed ones in the bulk samples of ALH-77231.

	Ni(%)	Au	Ir	Co	As
*Calculated	1.03	0.147	0.524	681	1.47
Analyzed	1.31±0.03	0.147±0.006	0.512±0.008	586±4	1.07±0.14

*Using 0.096 as a weight ratio of M-1 to non-magnetic fraction.

Table 5. Siderophile elements in metallic phases of ALH-77231.

Element	Bulk metal#	Taenite-rich fraction*	Taenite-rich fraction /bulk metal
Cu	626	4270	6.8
Ni(%)	9.98	36.0	3.6
Rh	1.5	5.68	3.8
Ge	41	146	3.6
Sb	0.61	2.1	3.4
Co	6840	2990	0.44
As	16.7	15.0	0.90
Re	0.512	1.33	2.6
Os	5.02	12.6	2.5
Ir	4.65	12.8	2.7
Pt	8.4	17.5	2.1
Au	1.66	4.79	2.9

#: M-1.
*: Weighted mean values of M-2, M-3 and M-4.

divided by those in M-1. The results in Table 5 show the following features for the metallic phases of the ALH-77231 (L6) chondrite.

Cu Cu is highly enriched in taenite; 6.8 times higher than that in M-1. As pointed out previously, the enrichment of Cu may be the result of precipitation during the dissolution of kamacite. RAMBALDI (1976) studied the Cu distributions between taenite and kamacite in L-group chondrites using size-separated metals. His results showed that the content ratio of Cu between taenite and kamacite was higher than that of Ni. The enrichment of Cu in the taenite of ALH-77231 is therefore an indigenous feature, although the possibility of partial reprecipitation of Cu cannot be ruled out.

Re, Os, Ir, Au These four elements are equally enriched in taenite compared with those in the M-1 fraction. Relative abundances of siderophile elements between each Ni-rich metal fraction (M-2, M-3 and M-4) consisting mainly of taenite and the bulk metal (M-1) are shown in Fig. 3. Re, Os and Ir are similarly distributed in the Ni-rich

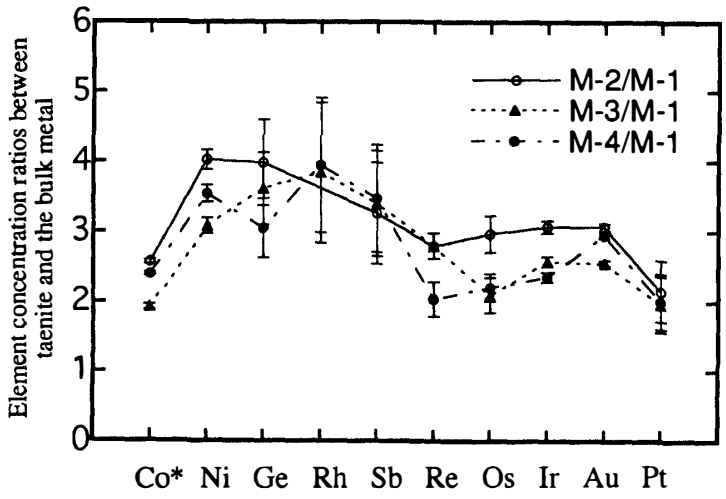

Fig. 3. Relative abundances of siderophile elements between taenite (M-2, M-3 and M-4) and the bulk metal (M-1). Among the siderophile elements shown in this figure, only Co is depleted in taenite and is inversely plotted as M-1/M-2, M-1/M-3 and M-1/M-4.

fractions but are not correlated with Ni. On the other hand, Au shows a good correlation with Ni. These results show that refractory siderophile elements, such as Re, Os and Ir, behave as a group.

Ni, Rh, Ge, Sb These four elements are all enriched in taenite to a similar extent.

Co The concentration of this element varies inversely with the Ni abundance in the metal grains of ordinary chondrites (SMITH *et al.*, 1993). In our data, Co contents are also inversely correlated with Ni in the three Ni-enriched metal fractions (M-2, M-3 and M-4) (Table 3 and Fig. 3), showing a similar trend to that found in taenite of L group chondrites (AFIATTALAB and WASSON, 1980).

As Arsenic is equally distributed in kamacite and taenite, showing no special affinity to either metal phase. This may imply either an equal migration of As in both metals after the separation of kamacite and taenite, or similar diffusion rates for As in the α-phase and γ-phase.

3.4. Element distributions between metal and non-magnetic fractions

Figure 4 shows the relative abundances of several elements between M-1 and bulk meteorite and between non-magnetic fraction and bulk meteorite for ALH-77231. It is evident that some Ir (about 20%) exists in the non-magnetic fraction. An apparent presence of Ir in non-magnetic phases of chondrites has been reported by other authors (RAMBALDI *et al.*, 1978; CHOU *et al.*, 1973) who pointed out, as in our results, that the ratios of Ir/Ni and Ir/Au are higher in non-magnetic silicates than those in bulk metal, suggesting that Ir in the non-magnetic fraction cannot be totally caused by the contamination of Fe-Ni metal. Ir/Ni and Ir/Au ratios in metal and non-magnetic fractions of ALH-77231 are given in Table 6. The Ir/Ni ratio in the non-magnetic portion is significantly higher than that in the bulk metal (M-1) or the

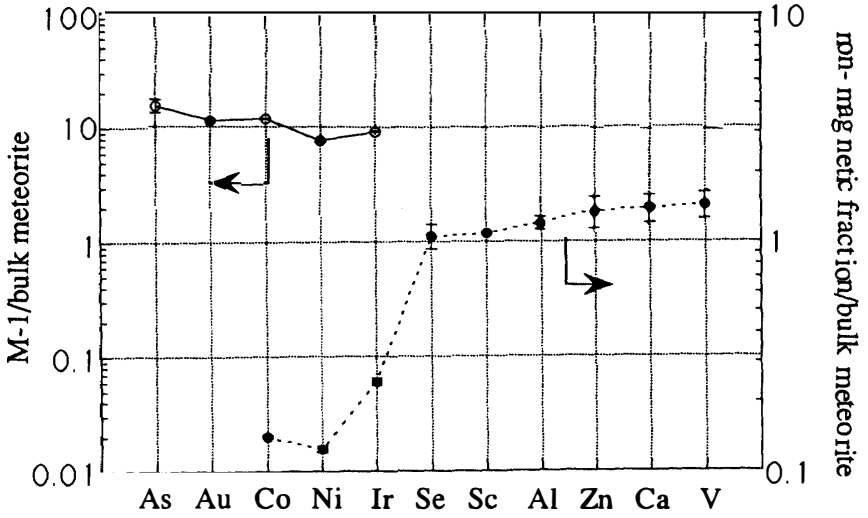

Fig. 4. Abundances of some elements in metal (M-1) and non-magnetic fractions of ALH-77231 relative to the bulk contents.

Table 6. Ir/Ni and Au/Ni ratios in separated phases of ALH-77231.

Content ratio ($\times 10^4$)	Bulk meteorite	M-1*	M-2#	Non-magnetic fraction
Ir/Ni	0.39±0.01	0.47±0.01	0.36±0.01	0.77±0.04
Au/Ni	0.112±0.005	0.166±0.005	0.127±0.004	<0.05

* Corresponds to bulk metal.
\# Corresponds to taenite.

Ni-rich taenite (M-2). Assuming that Ni in the non-magnetic fraction is attributable to fine-grained taenite (which might not have been efficiently separated), about 11% of the Ir can be assigned to the non-magnetic fraction.

While Os/Ir ratios of the metal fractions of ALH-77231 are in good agreement with the CI value, their Re/Ir ratios (0.10-0.12) are significantly higher than the CI value (0.076). If this fractionation is due to less effective agglomeration of CAI-like materials into the L chondrite parent body and no fractionation among Re and Ir occurred after the formation of the parent body, these CAI-like materials should be depleted in Re. However, such a process cannot explain the total fractionation of Re from Ir and Os, considering that the Re/Au ratio of M-1 (0.31) is also higher than the CI value (0.26). It is suggested that Re seems to be fractionated from Ir even in carbonaceous chondrites (ANDERS and EBIHARA, 1982), with the Re/Ir ratio being about 20% higher in CM than in CI chondrites. Even if a correction is made for a CI value of Re, fractionation of Re from Ir and Os between metal and non-metallic fractions needs still to be invoked. If a high temperature condensate, an analogue to the Allende CAIs, is present in the silicates, as suggested by CHOU *et al.* (1973), such a material should be depleted in Re relative to Ir and Os. The fractionation of Re from Ir and Os between metal and non-metallic fractions can be explained in terms of

either the later redistribution of Re between metal and non-metallic fractions or the difference in condensation behaviors of Re, and Ir and Os.

In the non-magnetic fraction of ALH-77231, the Ni and Co contents are significantly higher than their average values for the non-magnetic fractions of L-chondrites analyzed by RAMBALDI *et al.* (1978). According to equilibrium condensation calculations, Au is condensed after Fe-Ni metal, which is supported by a good correlation between Au and Ni in ordinary chondrites (LARIMER and WASSON, 1988). If the Ni in the non-magnetic fraction is attributable to ineffectively separated metals, its Au/Ni ratio should be in the range for M-1 and M-2. The Au distributions in the metal and the non-magnetic fractions of ALH-77231 are shown in Table 6. In the non-magnetic phase of ALH-77231, Au is obviously depleted relative to Ni; its content is even lower than the average value for the non-magnetic fractions of L-chondrites analyzed by RAMBALDI *et al.* (1978). This means that a portion of the Ni in the non-magnetic fraction of ALH-77231 is present as a non-metal component.

Acknowledgments

We are indebted to the reactor committee of the University of Tokyo for cooperative use of the reactor facilities of the Institute for Atomic Energy of Rikkyo University. C. KOEBERL and K. MISAWA are acknowledged for their critical reviews. This work is supported in part by a Grant-in-Aid for Scientific Research (No. 05453012 to M. E.) by the Ministry of Education, Science and Culture, Japan.

References

AFIATIALAB, F. and WASSON, J. T. (1980): Composition of the metal phases in ordinary chondrites: Implications regarding classification and metamorphism. Geochim. Cosmochim. Acta, **44**, 431–446.

ANDERS, E. and EBIHARA, M. (1982): Solar-system abundances of the elements. Geochim. Cosmochim. Acta, **46**, 2363–2380.

CHOU, C. L., BAEDECKER, P. A. and WASSON, J. T. (1973): Distribution of Ni, Ga, Ge and Ir between metal and silicate portions of H-group chondrite. Geochim. Cosmochim. Acta, **37**, 2159–2171.

CLARKE, R. S., Jr. and SCOTT, E. R. D. (1980): Tetrataenite-ordered FeNi, a new mineral in meteorites. Am. Mineral., **65**, 624–630.

GOLDSTEIN, J. I. and OGILVIE, R. E. (1965): The growth of the Widmanstätten pattern in metallic meteorites. Geochim. Cosmochim. Acta, **29**, 893–920.

GUTLICH, P., LINK, R. and TRAUTWEIN, A. (1978): Mössbauer Spectroscopy and Transition Metal Chemistry. Berlin, Springer, 247p.

HERPFER, M. A., LARIMER, J. W. and GOLDSTEIN, J. I. (1994): A comparison of metallographic cooling rate methods used in meteorites. Geochim. Cosmochim. Acta, **58**, 1353–1365.

HONDA, M., NAGAI, H. and SHIMAMURA, T. (1991): Trace elements in iron meteorites. Bull. Nat. Sci. Inst., Nihon Univ., **26**, 123–136.

JAROSEWICH, E., CLARKE, R. S., Jr. and BARROWS, J. N. (1987): The Allende Meteorite Reference Sample. Smithson. Contrib. Earth Sci., **27**, 49 p.

LARIMER, J. W. and WASSON, J. T. (1988): Siderophile element fractionation. Meteorites and the Early Solar System, ed. by J. F. KERRIDGE and M. S. MATTHEWS. Tucson, Univ. Arizona Press, 416-435.

LARSEN, L., ROY-POULSEN, H., ROY-POULSON, N. O. and VISTISEN, L. (1982): Order-disorder transitions in iron-nickel (50%-50%) alloys from iron meteorites as studied by Mössbauer spectroscopy. Phys. Rev. Lett., **48**, 1054–1056.

NARAYAN, C. and GOLDSTEIN, J. I. (1985): A major revision of the iron meteorite cooling rates—An experimental study of the growth of Widmanstätten pattern. Geochim. Cosmochim. Acta, **49**, 397–410.

RAMBALDI, E. R. (1976): Trace element content of metals from L-group chondrites. Earth Planet. Sci. Lett., **31**, 224–238.

RAMBALDI, E. R. (1977a): Trace element content of metals from H- and LL-group chondrites. Earth Planet. Sci. Lett., **36**, 347–358.

RAMBALDI, E. R. (1977b): The content of Sb, Ge and refractory siderophile elements in metals of L-group chondrites. Earth Planet. Sci. Lett., **33**, 407–419.

RAMBALDI, E. R., CENDALES, M. and THACKER, R. (1978): Trace element distribution between magnetic and non-magnetic portions of ordinary chondrites. Earth Planet. Sci. Lett., **40**, 175–186.

REUTER, K. B., WILLIAMS, D. B. and GOLDSTEIN, J. I. (1989a): Ordering in the Fe-Ni system under electron irradiation. Metall. Trans., **20A**, 711–718.

REUTER, K. B., WILLIAMS, D. B. and GOLDSTEIN, J. I. (1989b): Determination of the Fe-Ni phase diagram below 400°. Metall. Trans., **20A**, 719–725.

SAIKUMAR, V. and GOLDSTEIN, J. I. (1988): An evaluation of the methods to determine the cooling rates of iron meteorites. Geochim. Cosmochim. Acta, **52**, 715–726.

SCORZELLI, R. B., AZEVEDO, S., ORTLLI, I., PEDRAZZI, G. and BONAZZI, A. (1994): Iron-nickel superstructure in metal particles of Alfianello meteorite. Hyperfine Interactions, **83**, 479–482.

SCORZELLI, R. B., AZEVEDO, I. S., PEREIRA, R. A. PEREZ, C. A. C. and FERNANDES, A. A. R. (1993): Mössbauer spectroscopy study of the metallic particles of the Antarctic L6 chondrite ALH-769. Papers Presented to the 18th Symposium on Antarctic Meteorites, May 31–June 2, 1993. Tokyo, Natl Inst. Polar Res., 186–188.

SMITH, D. W., MIURA, Y. and LAUNSPACH, S. (1993): Fe, Ni and Co variations in the metals of some Antarctic chondrites. Earth Planet. Sci. Lett., **120**, 487–498.

WOOD, J. A. (1967): Chondrites: Their metallic minerals, thermal histories and parent planets. Icarus, **6**, 1–49.

(Received August 14, 1994; Revised manuscript received January 20, 1995)